ESD-TDR-64-333

Technical Report 355

Nondestructive Readout Scheme for Thin Film Memories

M. S. Maltz

21 May 1964

Prepared under Electronic Systems Division Contract AF 19(628)-500 by

Lincoln Laboratory
MASSACHUSETTS INSTITUTE OF TECHNOLOGY
Lexington, Massachusetts

The work reported in this document was performed at Lincoln Laboratory, a center for research operated by Massachusetts Institute of Technology, with the support of the U.S. Air Force under Contract AF 19(628)-500.

MASSACHUSETTS INSTITUTE OF TECHNOLOGY

LINCOLN LABORATORY

NONDESTRUCTIVE READOUT SCHEME FOR THIN FILM MEMORIES

M. S. MALTZ

Group 23

TECHNICAL REPORT 355

21 MAY 1964

LEXINGTON MASSACHUSETTS

NONDESTRUCTIVE READOUT SCHEME FOR THIN FILM MEMORIES*

ABSTRACT

If a magnetic bit in a thin film memary array is driven in the hard directian, the changing flux praduces eddy currents in the surraunding canducting surfaces. It has been pointed aut by Pahm and athers that the eddy field praduced by these currents always tends ta restare the bit magnetizatian ta its original direction. If this eddy field were strang enaugh at the end of the ward drive pulse, the effect cauld be made the basis af a scheme far nandestructive readaut (NDRO).

Same experiments were perfarmed an structures where the eddy field was strang enaugh ta restare the bit. The thin film plane used cantained 50 × 50-mil × 500-Å-thick Permallay films with uniaxial anisatrapy. The word line was campletely wrapped araund the plane. Ward-line-ta-ward-line spacings of 11.25 and 7.25 mils, and ward-line widths af 50, 75, and 150 mils were used. The eddy field wos measured at 50 ond 100 nsec after the switching aperatian ond, assuming an exponential eddy field decay, a time canstant was calculated.

Twa thearetical appraximatians were cansidered. In bath, the eddy currents were assumed ta flaw anly in the ward lines. In ane, the thickness af the lines was assumed negligible. In the other appraximatian, the thickness af the striplines was cansidered, but was assumed ta be af infinite width. The finite width, thin stripline approximatian seems ta be in better agreement with the measured values af the time canstant which varies between 76 and 200 nsec.

Accepted far the Air Farce
Franklin C. Hudsan, Deputy Chief
Air Farce Lincoln Labaratory Office

*This report is based an a thesis af the same title submitted ta the Department af Electrical Engineering at the Massachusetts Institute af Technalagy an 19 August 1963, in partial fulfillment of the requirements far the degree af Master of Science.

TABLE OF CONTENTS

	Abstract	iii
I.	Introduction	1
II.	Magnetic Thin Film Memories	2
III.	Theory	3
IV.	Experimental Apparatus	15
V.	Experimental Procedure and Results	19
VI.	Suggestions for Further Study	23
Appendix A		27
Appendix B		28

NONDESTRUCTIVE READOUT SCHEME FOR THIN FILM MEMORIES

I. INTRODUCTION

In recent years, much attention has been given to magnetic thin film structures, particularly for memory devices. Most of these devices use thin film bits of Permalloy, vacuum evaporated in a magnetic field, to give the resultant film uniaxial anisotropy. A few small memories have been manufactured commercially.

The basic advantage of magnetic thin films is that they switch much faster than ferrite devices. Because of the thinness of the film, the bit tends to exist in a single domain. Under the influence of short, powerful, driving fields, the entire magnetic spin system of the bit rotates as a unit, held together by the strong exchange interactions between the atomic spins. Therefore the bit switches, for fields above a certain threshold, by coherent rotation (a fast process which can be complete in nanoseconds) rather than by wall nucleation and motion, a much slower process.

It has been found possible to obtain nondestructive readout (NDRO) from thin films by limiting the drive fields to small values.[1] Unfortunately, the signals from the memory array are then quite small. Also, the information stored by the bit is susceptible to processes which gradually destroy the information. Recently, another technique (suggested by Pohm[2] and others) involves passive loading of the thin film bit. The currents induced in the passive loading structures when the film is switched produce fields which restore the bit to its original state at the end of the read operation. Eddy-NDRO is much less susceptible to gradual information destruction than drive-limited NDRO. Furthermore, much larger drive fields may be used and, therefore, much larger signals may be obtained from the films.

An understanding of the details of eddy-NDRO requires a thorough analysis of the interaction between the film and the eddy fields produced by the film. Pohm surrounds his bit with a shorted copper turn, thus making the analysis quite straightforward. It would be much more practical, however, if the passive loading could be produced by the striplines used for driving the bit. In this case, the analysis would be much more complex. Although Smay[3] did some rough calculations concerning this, it was found that a much more precise and rigorous procedure was needed to adequately handle the problem.

The work presented in this report has been directed, basically, toward an understanding of some of the details of the interaction between the eddy currents and the film. Most of the effort was devoted to a consideration of the time constant of the eddy current decay. Some equations for the calculation of the time constants were developed and compared with some experimental results.

II. MAGNETIC THIN FILM MEMORIES

The formation of Bloch walls is energetically unfavorable in very thin magnetic films.[1] Therefore, the magnetic bit can usually be considered as a single domain. It is important to note that under suitable conditions the film can break up into a multidomain structure.

If the film is evaporated with a magnetic field parallel to the plane of the substrate, the resultant film will have an axis of anisotropy in the direction in which the original field had been pointed. The magnetization of the film normally points along the anisotropy axis in either of the two possible orientations. As the magnetization vector is rotated away from the anisotropy axis, in the plane of the film, the energy of the film goes as $k \sin^2 \Lambda$, where Λ is the angle between the magnetization and the anisotropy axis, and k is the anisotropy constant. This contribution to the energy of the system is called the anisotropy energy. It gives rise to a torque, called the anisotropy torque, which tends to rotate the magnetization vector back into the anisotropy axis orientation through the smaller angle. This torque is zero at the unstable equilibrium at $\Lambda = 90°$.

A common memory structure is shown in Fig. 1. With no field applied, the magnetization of the bit can point in either direction along the easy axis, the name normally given to the anisotropy axis. The word lines produce a field, in the hard direction, which rotates the magnetization of the bit until it points in the hard direction. The resultant change in flux linking the sense line produces the output voltage, which is positive or negative depending upon the original direction of the bit magnetization. Information can be written into the bit by first rotating the magnetization into the hard direction. While the bit pulse is on, the word pulse is removed and the bit magnetization rotates back toward the anisotropy axis, pointing in the direction chosen by the bit field.

Real systems have certain imperfections which must be discussed. First, the direction of the anisotropy axis differs slightly from point to point through the film. In the film on which most of the experimentation was done, for example, 90 percent of the magnetization is within

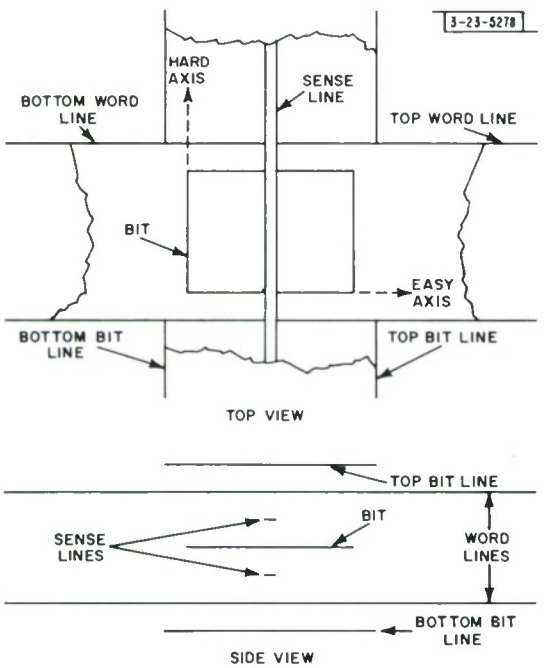

Fig. 1. Thin film memory bit, simplified view.

an anisotropy axis spread of 4.6°. To obtain good writing, the field in the easy direction must be strong enough to rotate most of the magnetization to either one side or the other of the $\Lambda = 90°$ point so that, upon the removal of the word drive, most of the magnetization will fall back to the easy axis pointing in the same direction. The spread in anisotropy axis is called dispersion.

Also, it is often impossible to align the word lines so that they are precisely parallel to the easy axis of the bit, since the direction of the easy axis varies for the various bits in the plane (this is known as skew). Although the skew angle is small, the word drive is quite large. This means that the component of the word drive along the easy axis may be appreciable. For good writing, the field in the easy direction must be large enough to overcome both skew and dispersion.

In the normal, destructive readout (DRO) mode, the bit breaks up into a multidomain structure at the end of the word pulse on a read operation. The part of the magnetization pointing to the left of the hard axis ($\Lambda = 90°$) falls back to the left, and the part of the magnetization pointing to the right of the hard axis falls back so that it points to the right along the easy axis. The information read out is then rewritten into the bit. Actually, the bit is never a truly one-domain structure, because there are usually small walls formed around impurities and at the edges of the bit.

The film can be operated in a current-limited NDRO mode by keeping the word current too small to ever bring the magnetization vector close to the hard axis. This restricts us to small sense line signals. Another limitation arises from the fact that writing a bit produces an easy direction field in all the bits along the bit line, including those not being written. This field may cause the small domains in the unselected bits to grow until, after many such operations, the information in the unselected bit is destroyed. Occasional reading and rewriting of the bits, as we do in the DRO mode, helps to alleviate this problem.

To operate in the eddy-NDRO mode, the eddy field (produced when the bit is driven into the hard direction) must be strong enough to overcome skew and dispersion and restore the bit to its original condition when the word pulse is removed. In the time between the rise and fall of the word pulse, the eddy field will be rapidly decaying; therefore, the word pulse must be quite short. However, its amplitude may be made large enough to obtain the full, DRO sense line signal.

It is conceivable that the eddy field might even be able to regenerate a partially broken-up bit. If, for example, the eddy field produced from a bit, of which 10 percent had broken up, was strong enough to restore 91 percent of the magnetization, the signal would gradually improve with successive NDRO operations.

III. THEORY

An analysis of eddy-NDRO naturally falls into two parts. First, we must find out how the eddy field produced by the bit behaves and, second, we must find out how this field affects the bit.

The rotational time constant of the isolated film is on the order of one or two nanoseconds, so it can be assumed that the film will respond instantaneously to the applied fields. The applied fields, however, are not uniform and, therefore, different portions of the film spin system experience different torques. The exchange forces are fairly large; therefore, we assume that the film magnetization rotates as a unit under an average torque produced by an average field. If

the magnetization attempted to rotate out of the plane of the film, we would have free poles on the upper and lower surfaces of the film. This would produce a very large field outside the bit. This field would have a large energy. Therefore, the magnetization vector is constrained to rotate in the plane of the film. For our square bits, the angle of the magnetization to the easy axis is, to a good approximation, the equilibrium angle between the torques due to the applied fields, including the eddy field, and the torque due to the anisotropy.

Suppose the magnetization per unit volume is u. Then, the torque upon the spin system when the magnetization has rotated an angle Λ from the easy axis is (see Fig. 2) $uH_y \cos\Lambda - uH_x \sin\Lambda$. The anisotropy energy is $k \sin^2\Lambda$, where k is the anisotropy constant. Therefore the torque is $-k \sin 2\Lambda$; $\overline{M} = u(l_x \cos\Lambda + l_y \sin\Lambda)$. As a result, the value of $d\overline{M}$ is $u(l_y \cos\Lambda - l_x \sin\Lambda)\,(d\Lambda/dt)\,dt$. The eddy field at time t due to a change in the magnetization at time p will be some function of $t - p$; $d\overline{H}_e = -Bd\overline{M}f(t-p) = -Bf(t-p)\,u(l_y \cos\Lambda - l_x \sin\Lambda)\,(d\Lambda/dp)\,dp$. The total torque T due to the eddy currents at time t is

$$T = -Bu^2 \left[\cos\Lambda \int_o^t (d\Lambda/dp) \cos\Lambda\, f(t-p)\, dp + \sin\Lambda \int_o^t (d\Lambda/dp) \sin\Lambda\, f(t-p)\, dp\right] .$$

We can integrate by parts to put the equation in a more usable form. For example, if we are considering a turn-on problem, where Λ at time zero is zero

$$T = -Bu^2 \left\{\cos\Lambda \left[\sin\Lambda - \int_o^t \sin\Lambda\,(df/dp)\, dp\right] + \sin\Lambda \left[-\cos\Lambda + f(t) + \int_o^t \cos\Lambda\,(df/dp)\, dp\right]\right\} . \tag{1}$$

We chose B so that f(0) is one. If the drive is a word pulse in the y-direction (H_y),

$$uH_y \cos\Lambda = -T + k \sin 2\Lambda \quad ; \tag{2}$$

f(t) is probably quite close in form to that of a decaying exponential. Once we find it (and B), it is quite simple to integrate the preceding equations to find the dependence of Λ on time.

If the word drive is strong enough to rotate the bit magnetization into the hard direction in a time which is much less than the decay time of f(t), we need not do the integrals at all. We merely need to find the eddy field produced by reducing the x-component of $\overline{M}$ suddenly to zero and increasing the y-component of $\overline{M}$ suddenly to u. We are basically interested in the changes in $\overline{M}$ and $\overline{H}_e$ in the easy direction.

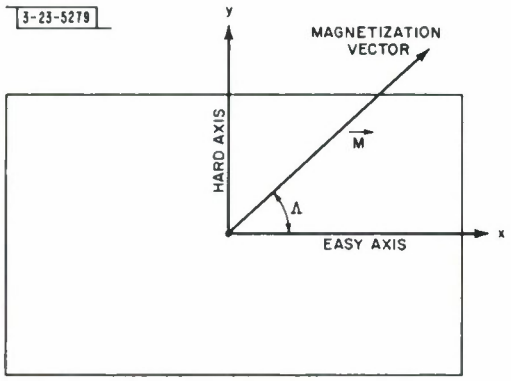

Fig. 2. Bit coordinate axes.

It is now neeessary to find the eddy field produced by a ehange in the film magnetization. First, the normal modes of deeay will be found. A normal mode is a field distribution whose time dependence is completely eontained in a multiplieative faetor of $\exp[-st]$. We know that, immediately after the magnetization ehange, an eddy eurrent will flow to keep the field in the copper constant. This transient eurrent, and the transient field it produees, will gradually go to zero as the field pattern goes to its new steady state. We ean write the transient field as the sum of normal modes, and thereby ealeulate the behavior of the field with time.

Under the assumption of exponential deeay, Maxwell's equations outside the film become

$$\nabla \times \bar{H} = \frac{4\pi \bar{J}}{c} \qquad \nabla \times \bar{E} = \frac{s}{c} \bar{H}$$

$$\nabla \cdot \bar{H} = 0 \qquad \nabla \cdot \bar{E} = -4\pi\rho_c \quad .$$

We have ignored the displaeement current eompared with the conduction current. Where ρ is the resistivity of the copper, $\bar{E} = \rho \bar{J}$. Therefore, inside the copper

$$\nabla^2 \bar{H} = -\frac{4\pi s}{\rho c^2} \bar{H}$$

$$\nabla \cdot \bar{H} = 0 \quad .$$

Outside the copper

$$\nabla^2 \bar{H} = 0 \quad ,$$

$$\nabla \cdot \bar{H} = 0 \quad .$$

The current normal to any copper-air surfaee must be zero.

The eddy currents in the sense lines produee a negligible field, sinee the sense lines are so small. Therefore, we ean approximate our structure by that shown in Fig. 3. The eddy currents

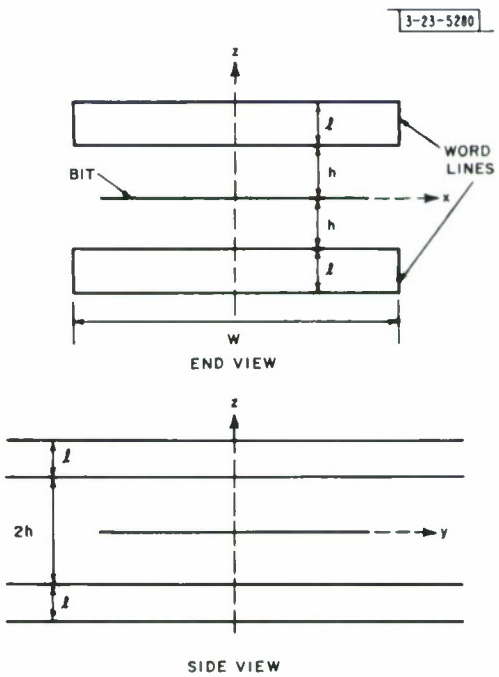

Fig. 3. Copper structure for eddy-current calculations.

in the bit itself are assumed negligible, since it is extremely thin. The easy axis is in the y-direction. The striplines extend to plus and minus infinity in the y-direction. As a further simplification, we look only for those modes which are symmetrical about the z = 0-plane, which amounts to assuming that the film is in the exact center of the stripline structure.

The problem, as stated, is fairly difficult. First, we will solve the simpler problem in which the striplines are replaced by infinite copper sheets, and W goes to infinity. We can solve the partial differential equations involved by separation of variables. We assume a solution of the proper form for each of the three regions involved (copper, air between lines, air outside of lines) and apply boundary conditions. Region one is the volume outside the lines. Assume that

$$H_z = H'_{oz} \exp[-a'z] \sin(by) \cos(gx) \quad .$$

In order to satisfy the divergence condition on H (that it be zero),

$$H_x = H'_{ox} \exp[-a'z] \sin(by) \sin(gx) \quad ,$$

$$H_y = H'_{oy} \exp[-a'z] \cos(by) \cos(gx) \quad .$$

Applying the condition that the divergence equal zero,

$$-a'H'_{oz} - bH'_{oy} + gH'_{ox} = 0 \quad .$$

Since the Laplacian of H must also equal zero,

$$a'^2 = b^2 + g^2 \quad .$$

In region two (the volume inside the copper),

$$H_z = H''_{oz} \sin(a''z + n) \sin(by) \cos(gx) \quad ,$$

$$H_x = H''_{ox} \cos(a''z + n) \sin(by) \sin(gx) \quad ,$$

$$H_y = H''_{oy} \cos(a''z + n) \cos(by) \cos(gx) \quad ,$$

$$a''H''_{oz} + gH''_{ox} - bH''_{oy} = 0 \quad ,$$

$$a''^2 + b^2 + g^2 = \frac{4\pi s}{\rho c^2} \quad .$$

In region three (the volume between the striplines),

$$H_z = H'''_{oz} \sinh(a'''z) \sin(by) \cos(gx) \quad ,$$

$$H_x = H'''_{ox} \cosh(a'''z) \sin(by) \sin(gx) \quad ,$$

$$H_y = H'''_{oy} \cosh(a'''z) \cos(by) \sin(gx) \quad ,$$

$$a'''^2 = b^2 + g^2 = a'^2 \quad ,$$

$$a'H'''_{oz} + gH'''_{ox} - H'''_{oy} = 0 \quad .$$

The z-component of the current must equal zero at z = h and z = h + ℓ .

$$1_z(\nabla \times \bar{H}) = 0 = \frac{\partial H_y}{\partial x} - \frac{\partial H_x}{\partial y} \quad ,$$

$$0 = (H''_{oy} g + b H''_{ox}) \cos(a''z + n) \cos(by) \sin(gx) \quad .$$

Either

$$\cos(a''h + n) = 0 \quad ,$$

$$\cos[a''(h + \ell) + n] = 0 \quad ,$$

or

$$H''_{oy} g + b H''_{ox} = 0 \quad .$$

The first condition does not interest us, since it corresponds to H_x and H_y equal to zero at the copper-air boundaries.

At the boundaries, $\bar{H}$ must be continuous. This last condition gives us a set of simultaneous equations which we can solve (see Appendix A). Deriving an equation for the relation between a' and a'', we find

$$a'a'' [\tanh(a'h) + 1] = [a''^2 \tanh(a'h) - a'^2] \tan(a''\ell) \quad . \tag{3}$$

This equation can be solved numerically. Note that a'' is a multivalued function of a'. We may now plot s as a function of a' and a''. A set of normalized curves is presented in Fig. 4. For given values of b and g, the mode with the lowest value of s is called the fundamental mode. Note that the first higher order mode has a much greater value of s than the fundamental mode. Since s is the inverse of the time constant, the higher order modes (and modes with large values of b and g) die out very quickly. Therefore, after a short time the characteristic time constant of decay will be the value for the fundamental mode with a' equal to zero. Therefore,

$$1/h = a'' \tan(a''\ell) = a''^2 \ell$$

if $a''\ell$ is small. This turns out to be true. Therefore, to a good approximation,

$$\frac{1}{h\ell} = \frac{4\pi s}{\rho c^2} \quad . \tag{4}$$

Consider a sudden change of bit magnetization in the y-direction at time zero. At time zero-plus, the field in the copper has not changed, so we must write the difference between the static bit field in the copper before and after the change (the transient field) as a superposition of the normal modes which we have found. Since we know the time dependence of each normal mode, we can find the time dependence of the eddy field as it decays toward zero. In particular, we are very interested in the magnitudes of the lower modes, since the higher ones quickly die out. The lower modes represent slow variations of the fields with the space variables. Figure 5 is a sketch of the fundamental and first higher order modes for small values of b and g. For the static bit field, the variation of H_z between z = h and z = h + ℓ is not particularly great if h is greater than ℓ. For the nonfundamental modes, the variation of H_z with z is extreme. We therefore expect the coefficients of the nonfundamental modes to be small in our linear superposition. The variation of H_z with x and y, however, is much more extreme, since most of the static bit field penetrates the copper in a small region around the poles of the bit. Therefore, the coefficients of modes with large values of b and g are large. This tells us that much

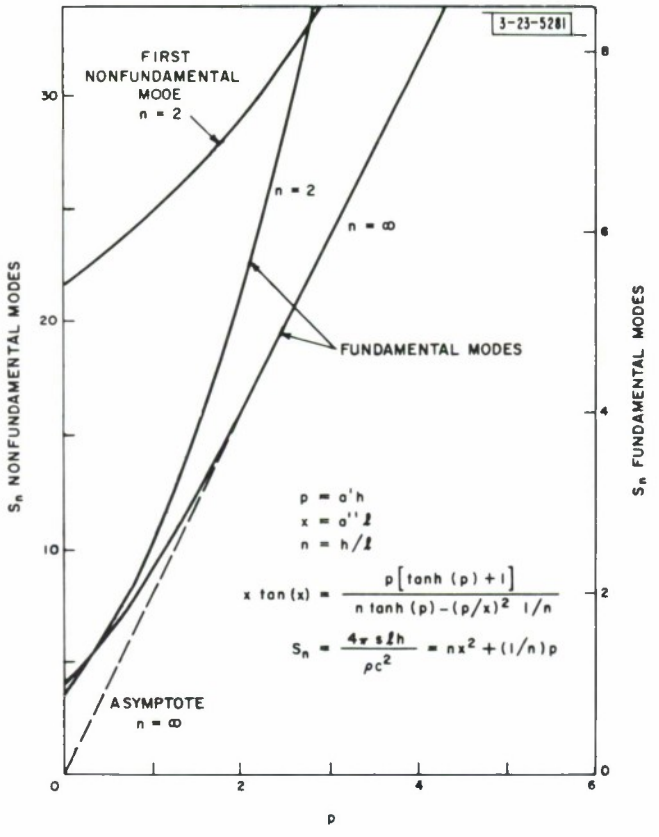

Fig. 4. Graph of normalized inverse time canstant (Sn) vs normalized wavelength.

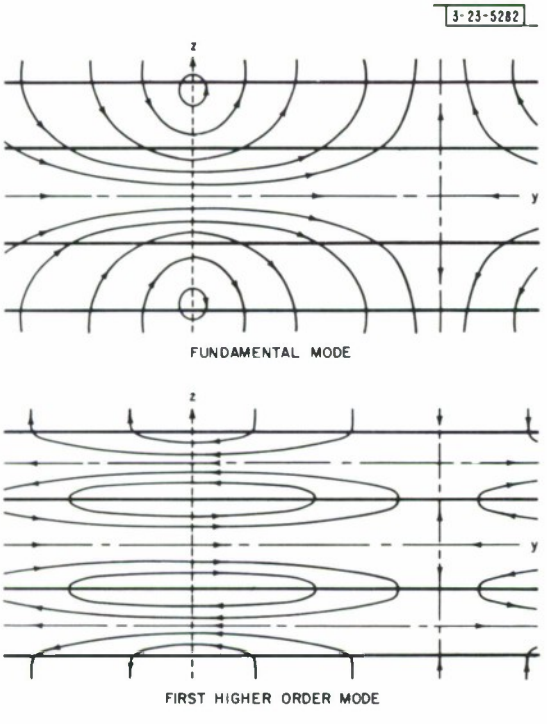

Fig. 5. Normal mades af thick, infinite sheet theary.

of the flux participates in a fast decay process, and only a small portion of the flux goes into the slowly decaying modes.

This makes much physical sense. The high concentration of the static bit field near the poles of the bit requires a high concentration of current near the poles to keep the field penetrating the copper at time zero-plus the same as it was at time zero-minus. This produces very high $J^2\rho$ losses, a rapid rate of dissipation of energy, and therefore a rapid decay. In the modes with small values of a', the current distribution is much less concentrated and, therefore, the energy dissipation and decay rate are much smaller.

An attempt was made to find the coefficients of the modes by hand calculation. It was concluded that an adequate calculation could only be done by computer, since the characteristic "spectrum" for a reasonable magnetic thin film configuration is very complex.

A similar calculation can be performed for a single sheet of copper. We find that

$$a' = a'' \tan(a''\ell/2) \quad , \tag{5}$$

$$a'^2 + a''^2 = \frac{4\pi s}{\rho c^2} \quad . \tag{6}$$

For a' smaller than $1/h$, which is the case for the slowly decaying modes, the single-sheet time constant is much longer than the double-sheet time constant. This again makes physical sense, since the field in the single-sheet case is much more extensive than in the double-sheet case. Therefore, there is more field energy stored in the single-sheet $\bar{H}$ field than in the double-sheet $\bar{H}$ field for the same current densities and energy dissipation rates.

As the width of the stripline approaches the width of the bit, the validity of the infinite sheet theory becomes questionable. However, the theory is still not completely unreasonable, since the aspect ratio between the line widths and their spacing is still quite large. It would be very desirable, however, to have a theory that explicitly took the width of the striplines into account.

To make the problem tractable, we assume that the striplines are thin sheets and that the current is uniform across them. This means that only the time derivative of H_z is effective in producing a current. Because of this assumption, we only find modes similar to the fundamental modes of the infinite sheet theory. Once again, when we have found the normal modes, we will write H_z as a linear superposition. Many techniques were tried in order to solve the problem. The one finally chosen is fairly straightforward, though laborious.

We can find the value of H_z by integration over the currents of the sheet. We consider $\bar{J}$ as a surface current, and ρ as a surface resistivity (bulk resistivity/thickness):

$$H_z = \frac{1}{c} \iint \frac{J_x(y - y') - J_y(x - x')}{[(y - y')^2 + (x - x')^2 + (z - z')^2]^{3/2}} \, dx' \, dy' \quad ,$$

$$H_z = (\nabla \times \bar{J}) \cdot \bar{1}_z \, \frac{\rho c}{s} \quad \text{(at the planes)} \quad . \tag{7}$$

The integration must be performed over both the upper and lower planes. We now assume a form for the currents in the plane. We assume that the current in the lower plane is the negative of the current in the upper plane, by symmetry. Since $\bar{H}$ must be a symmetric function of x, the current in the y-direction must be antisymmetric in x. The x-component of the current must be zero at $x = \pm W/2$. We chose to represent $\bar{J}$ by a trigonometric series, so J_y goes as $\sin(Nx)$. $\sin(n\pi x)$ forms a complete set from zero to one; $\sin(2n + 1)\pi x$ is symmetric about $\frac{1}{2}$, while $\sin(2nx\pi)$ is antisymmetric about $\frac{1}{2}$. We move the origin of the set to $\frac{1}{2}$ for convenience.

An assumed $\bar{J}$, which satisfies the symmetry requirements in the upper sheet, has its divergence equal to zero, and has a J_x-component equal to zero at $x = \pm W/2$ is

$$\bar{J} = \sum_{n=0}^{\infty} A_n [1_y \sin(Nbx/g) \sin(by) + 1_x (g/N) \cos(Nbx/g) \cos(by)] \quad , \tag{8}$$

where

$$N = (2n + 1)\pi \quad ,$$

and

$$g = bW \quad ,$$

$$\bar{1}_z (\nabla \times \bar{J}) = \sum_{n=0}^{\infty} A_n \left(\frac{Nb}{g} + \frac{gb}{N}\right) \cos(Nbx/g) \sin(by) \quad . \tag{9}$$

Note that we have not summed over b. This assumes that a normal mode has a sinusoidal variation in the y-direction. To show that this is true, consider the integral for the field in the upper half plane produced by the currents in the lower half plane (note, $m = 2h$),

$$\frac{1}{c} \sum_{n=0}^{\infty} A_n \int_{-\infty}^{+\infty} dy' \int_{-W/2}^{W/2} dx' \frac{[\sin(Nbx'/g) \sin(by')] (x - x') - \frac{g(y - y')}{N} \cos\left(\frac{Nbx'}{g}\right) \cos(by')}{[(y - y')^2 + (x - x')^2 + m^2]^{3/2}} \quad . \tag{10}$$

Consider the y-dependence of the first term of the integrand. Make the transformation $y - y' = \nu$, and $dy' = -d\nu$. Thus,

$$\int_{-\infty}^{+\infty} \frac{\sin(by')\, dy'}{[(y - y')^2 + (x - x')^2 + m^2]^{3/2}} = \sin(by) \int_{-\infty}^{+\infty} \frac{\cos(b\nu)\, d\nu}{[\nu^2 + (x - x')^2 + m^2]^{3/2}} \quad , \tag{11}$$

and

$$\int_{-\infty}^{+\infty} \frac{(y - y') \cos(by')\, dy'}{[(y - y')^2 + (x - x')^2 + m^2]^{3/2}} = \sin(by) \int_{-\infty}^{+\infty} \frac{\nu \sin(b\nu)\, d\nu}{[\nu^2 + (x - x')^2 + m^2]^{3/2}} \quad . \tag{12}$$

By a change of variables, we may write the above expressions so that they involve integrals with only one variable parameter:

$$\lambda = \sqrt{m^2 + (x - x')^2} \quad ,$$

and

$$L = \nu/\lambda \quad .$$

Equations (11) and (12) become, respectively,

$$\frac{\sin(by)}{\lambda^2} \int_{-\infty}^{+\infty} \frac{\cos(b\lambda L)\, dL}{(1 + L^2)^{3/2}} = \frac{\sin(by)\, 2Co(b\lambda)}{\lambda^2} \quad , \tag{13}$$

and

$$\frac{\sin(by)}{\lambda} \int_{-\infty}^{+\infty} \frac{L \sin(b\lambda L)\, dL}{(1 + L^2)^{3/2}} = \frac{\sin(by)\, 2So(b\lambda)}{\lambda} \quad , \tag{14}$$

where

$$Co = \int_o^\infty \frac{\cos(b\lambda L)\, dL}{(1 + L^2)^{3/2}} \quad ,$$

$$So = \int_o^\infty \frac{L \sin(b\lambda L)\, dL}{(1 + L^2)^{3/2}} \quad .$$

Note that the derivative of Co(x) with respect to x is −So(x).

Set (7) equal to $(\nabla \times \bar{J}) \cdot \bar{1}_z \rho c/s$. We now multiply both sides of the expression by cos(Qbx/g) and integrate from −W/2 to +W/2. Since the cosines are orthogonal in the interval from −W/2 to +W/2, we find that, after dividing out the sin(by) dependence from both sides and some manipulating (for full details see Appendix B), the following expression must hold for all values of q:

$$\frac{\rho c^2 Q b^2}{2s} \left[1 + \left(\frac{g}{Q}\right)^2\right] A_q = \sum_{n=0} A_n H_{nq}(b) \quad , \tag{15}$$

where

$$H_{nq}(b) = H^l_{nq}(b) + H^u_{nq}(b) \quad ,$$

and

$$Q = (2q + 1)\, \pi \quad .$$

Both q and n take on all integral values, including zero. The expressions for $H_{nq}(b)$ are quite complicated. The expression $H^l_{nq}(b)$ arises from the contribution of the currents in the lower sheets to the field at the upper sheet, and $H^u_{nq}(b)$ arises from the contribution of the currents in the upper sheet to the field at the upper sheet.

The expression $H_{nq}(b)$ is described by one expression when n equals q, and by another expression when n is not equal to q:

$$H_{nq}(b) = 4 \int_o^g \frac{dk(-1)^{n-q}\, g}{(Q^2 - N^2)\, K\lambda^2} \left\{\frac{g}{N}\left[N \sin\left(\frac{Qk}{g}\right) - Q \sin\left(\frac{Nk}{g}\right)\right] Ds \right.$$

$$\left. + 2Q \sin\left(\frac{Q - N}{2g} k\right) \sin\left(\frac{N + Q}{2g} k\right) De\right\} \quad , \tag{16}$$

$$H_{qq}(b) = 4 \int_o^g \frac{dk}{k\lambda^2} \left[\frac{g}{Q} Ds(k, b)\, I(k) + \frac{k - g}{2} \sin\left(\frac{Qk}{s}\right) Dc(k, b)\right] \quad , \tag{17}$$

where

$$I(k) = \frac{g - k}{2} \cos\left(\frac{Qk}{g}\right) + \frac{g}{2Q} \sin\left(\frac{Qk}{g}\right) \quad ,$$

$$k = (x - x')\, b \quad ,$$

$$\lambda = \sqrt{(k/b)^2 + m^2} \quad ,$$

$$Ds(k, b) = b\lambda^2 So(k) - k\lambda So(b\lambda) \quad ,$$

$$Dc(k, b) = \frac{k^2}{b} Co(b\lambda) - b\lambda^2 Co(k) \quad .$$

For any value of b, the set of simultaneous equations described by (15), (16), and (17) have nontrivial solutions only for certain values of s. Corresponding to each one of these values of s and b, there is a normal mode of decay. We can solve for the values of s which give nontrivial solutions if we put (15) in matrix form,[4] i.e.,

$$M_{qn}A_n = 0 \quad ,$$

where

$$M_{qn} = H_{nq}(b) - \delta_{qn}\frac{\rho c^2 Q b^2}{2s}\left[1 + \left(\frac{g}{Q}\right)^2\right] \quad ; \tag{18}$$

$$\delta_{qn} = \begin{cases} 0 & q \neq n \\ 1 & q = n \end{cases} \quad .$$

There is a nontrivial solution for the set of equations only where the determinant of M_{qn} is equal to zero. The application of this condition will give us a polynomial in s to solve. For each root, we can solve for the coefficients A_n which describe the normal mode.

In order to make use of the results obtained, we must evaluate Co(x). By differentiation, So(x) may be found. Therefore, a numerical integration was performed and a few points plotted. It was found that an excellent fit could be obtained with a function consisting of the sum of two exponentials (see Fig. 6). For a more thorough evaluation, it is possible to write Co(x) as a sum of Legendre functions. The Legendre functions form a complete, orthonormal set,[5] from zero to infinity, with the general expression

$$V_n(x) = \sum_{i=0}^{i=n} C_{ni} \exp\left[-px\left(i + \frac{1}{2}\right)\right] \quad . \tag{19}$$

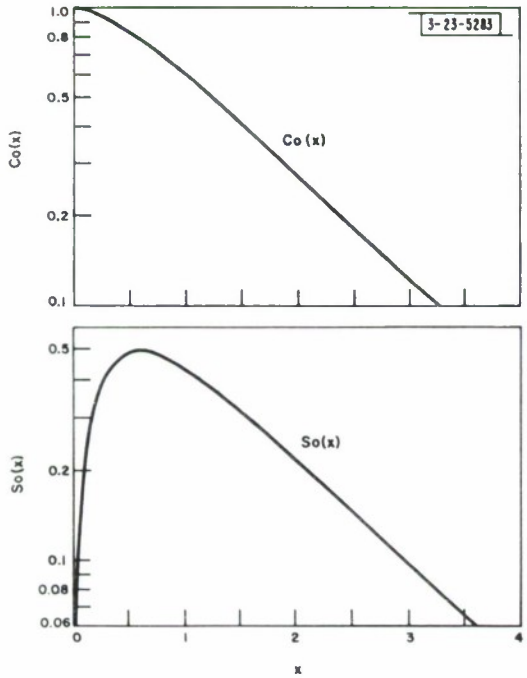

Fig. 6. Plots of So(x) and Co(x).

The coefficients C_{ni} are tabulated by Lee[5] and others. If we wish to express Co(x) as a linear superposition of V_n with coefficients D_n, we find D_n by integration, i.e.,

$$D_n = \int_o^\infty Co(x)\ V_n(x)\ dx = \int_o^\infty \int_o^\infty \frac{\sum_{i=0} C_{ni} \exp[-px(i + \frac{1}{2})] \cos(xy)\ dy\ dx}{(1 + y^2)^{3/2}} \quad . \tag{20}$$

Doing the x integral first,

$$\int_o^\infty \exp[-w_i x] \cos(xy)\ dx = \frac{w_i}{w_i^2 + y^2} \quad ,$$

where

$$w_i = p(i + \tfrac{1}{2}) \quad .$$

Equation (20) now becomes

$$D_n = \sum_{i=0}^{i=n} C_{ni} \int_o^\infty \frac{w_i\ dy}{(w_i^2 + y^2)\ (1 + y^2)^{3/2}} = \sum_{i=0}^{i=n} C_{ni} F(w_i) \quad . \tag{21}$$

The integral can be evaluated in closed form upon the substitution:

$$y = \frac{u}{\sqrt{1 - u^2}} \quad ,$$

$$\int_o^\infty \frac{w_i\ dy}{(w_i^2 + y^2)\ (1 + y^2)^{3/2}} = \int_o^1 \frac{w_i(1 - u^2)\ du}{w_i^2 + (1 - w_i^2)\ u^2} = F(w_i)$$

$$= \frac{w_i}{w_i^2 - 1} \left[1 - \frac{\ln\left(w_i^2 + \sqrt{w_i^2 - 1}\right) - \ln\left(w_i^2 - \sqrt{w_i^2 - 1}\right)}{2 w_i \sqrt{w_i^2 - 1}} \right] \qquad w > 1$$

$$= \frac{w_i}{w_i^2 - 1} \left[1 - \frac{\arctan\left(\frac{\sqrt{1 - w_i^2}}{w_i}\right)}{w_i \sqrt{1 - w_i^2}} \right] \qquad w < 1 \tag{22}$$

Knowing $F(w_i)$ in closed form, and knowing C_{ni}, we can find the coefficients D_n; p is chosen to give rapid convergence. This technique would be quite suitable for machine computation. It is inconvenient for hand computation because the functions V_n involve the small differences of large quantities.

A hand calculation was done, basically, to see if the results obtained were reasonable. Co(x) was approximated by

$$Co(x) = 1.35 \exp[-0.804\,x] - 0.35 \exp[-3.10\,x] \quad .$$

This expression has the proper value and slope at x = 0 and the correct asymptotic behavior for large x. We choose W to be 50 mils and h to be 7 mils. The wavelength of the sinusoidal

variation in the y-direction is chosen to be 100 mils. The bits we use are roughly 50 mils long; choosing this value of b puts the adjacent positive and negative peaks of the sinusoid over the north and south poles of the bit. We only consider the bottom two modes. Using an interval of 0.1 g, we do a numerical integration to calculate the values of the matrix components. The resultant matrix equation is

$$\begin{Bmatrix} 0 \\ 0 \end{Bmatrix} = \begin{Bmatrix} 0.503 - t(0.151) & +0.034 \\ +0.103 & 0.557 - t(0.251) \end{Bmatrix} \begin{Bmatrix} A_0 \\ A_1 \end{Bmatrix} ,$$

$$t = \frac{\rho c^2}{4\pi s} = \frac{\rho_b c^2}{4\pi \ell s} ,$$

$$\text{time constant} = \frac{4\pi \ell t}{\rho_b c^2} .$$

The bulk resistivity is ρ_b, the surface resistivity is ρ, and the thickness of the copper is ℓ.

The two solutions for t are 3.41 and 2.14. For convenience, t is measured in mils. Corresponding to the 3.41 solution, we find A_1 over A_0 to equal +0.345. Corresponding to the 2.14

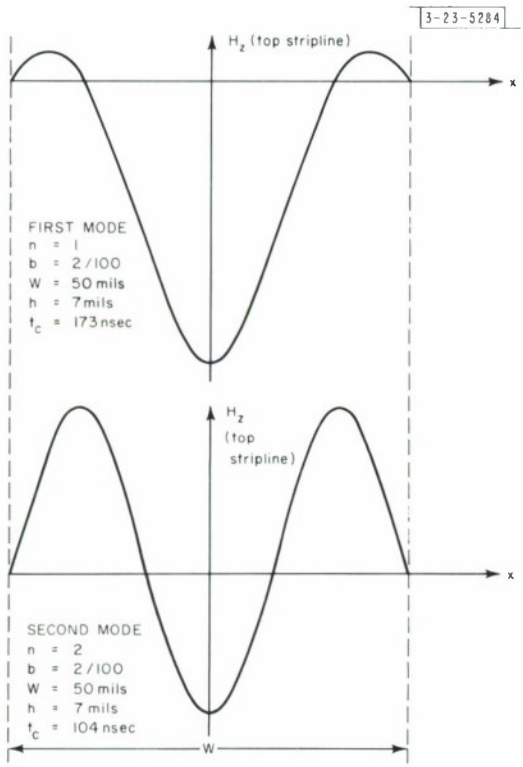

Fig. 7. Normal modes of thin, finite stripline theory.

solution, A_1 over A_0 is equal to −5.3. Assuming the thickness and resistivity to be the same as in our structure, we find the time constants to be 172 and 104 nsec. Plots of the x variation of H_z at the upper plane are shown in Fig. 7. They are quite different from the modes of decay one finds for the infinite sheet case.

For b = 0, the equations can be put in a much simpler form:

$$\frac{\rho e^2 Q}{2s} A_q = \sum_{n=0}^{\infty} A_n H_{nq}(0) \quad , \tag{23}$$

$$H_{nq}(0) = 8m^2 W \int_o^g \frac{dx(-1)^{n-q} Q \sin(\frac{Q+N}{2W} x) \sin(\frac{Q-N}{2W} x)}{x\lambda^2(N^2 - Q^2)} \quad ; \tag{24}$$

$$H_{qq}(0) = 2m^2 \int_o^g \frac{dx(W-x) \sin(\frac{Qx}{W})}{x\lambda^2} \quad . \tag{25}$$

The ratio between the widths of the striplines and their spacing is large enough (for all our configurations) so that the off-diagonal matrix elements are small enough to make a negligible change in the time constant. For example, if we merely set the diagonal elements of our matrix equal to zero, we would have obtained values of 3.34 and 2.22 for t. This compares very closely with the more accurate values of 3.41 and 2.14.

Taking only the diagonal matrix elements,

$$\frac{\rho e^2 Q}{2s} = H_{qq}(0) \quad ,$$

$$T_q = \text{time constant} = \frac{1}{s} = \frac{2H_{qq}(0)}{\rho Q e^2} \quad . \tag{26}$$

It is important to note that the modes we find for the same value of b are not orthogonal to each other.

IV. EXPERIMENTAL APPARATUS

In the experiments which were performed, driving currents were generally on the order of amperes, while the sense line output was on the order of a fraction of a millivolt. The rise and fall times of the drive pulse were quite short. As a result, the noise problem was exceedingly severe. With careful alignment and shielding, however, it was possible to increase the signal-to-noise ratio to three-to-one.

The configuration used is shown in Fig. 8. The bit line and the top word line are cut away to show the sense line and the bit. A side view of the sandwich is shown in Fig. 9. The dummy bit line was not connected electrically to any power source. It was used to obtain an estimate of the effect of the eddy currents flowing in the bit line upon the bit. It changed the measured eddy field by only 2 percent.

Three different word lines were used. The 75- and 150-mil-wide lines were both made from the same material. The thickness, as measured by a micrometer, was 2 mils. The more important parameter for our work, however, was the surface resistivity. This was found by measuring the resistance of a length of the stripline, and multiplying it by the ratio of width to length. The 50-mil-wide stripline was made of different material. Its thickness also measured 2 mils, but its surface conductivity was somewhat lower.

The sense line is different from the one shown in Fig. 1. This type of sense line is known as a planar sense line. It reduces the number of layers required between the word lines, so that they may be brought closer together. This type of sense line also decreases the coupling between the bit line and the sense line. With the structure shown in Fig. 1, a very large signal

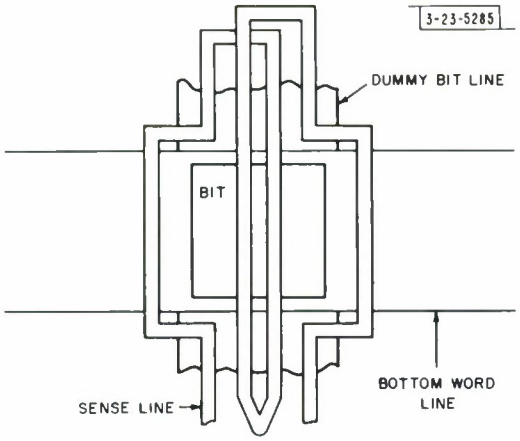

Fig. 8. Experimentol stripline configurotion, top view.

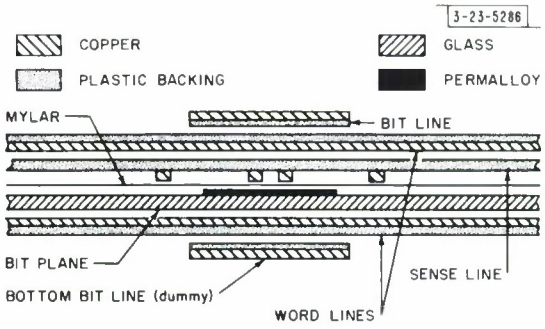

Fig. 9. Experimentol stripline configurotion, side view.

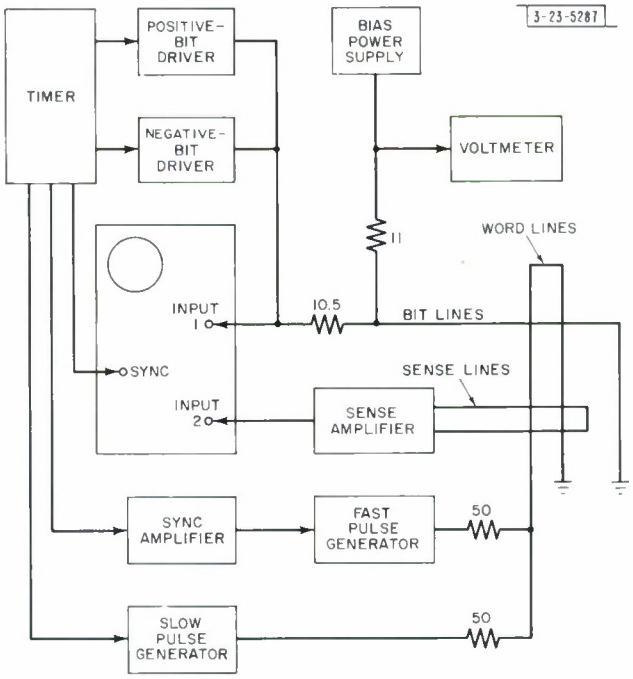

Fig. 10. Associoted electronics.

is coupled into the sense line during a write operation, and the sense amplifier may not be used again until it has recovered from the effects of the large pulse. The total thickness of the sense line and backing was found to be 4 mils.

The thin film plane used contained square bits 50 mils on a side. The inter-bit spacing was also 50 mils. The plane was originally 7 mils thick, giving a total word-line-to-word-line spacing of 11.25 mils. For the last part of the experiment, the glass plane was etched until it was only 3 mils thick, giving a total spacing of 7.25 mils.

The driving and sensing circuitry is shown in Fig. 10. The sense lines are connected to the sense amplifier with double-wire, shielded cable. The sense amplifier is a balanced difference amplifier with a gain of 100. The output of the sense amplifier is displayed on a Type 535 Tektronix oscilloscope which has a 53B plug-in unit. The rise time of the sense-amplifier-oscilloscope system was about 20 nsec. The sync amplifier, negative-bit driver, and slow word pulse generator used were all Lincoln Laboratory Model V standard pulse generators.[6] They are capable of driving a maximum of about 500 ma into a 50-ohm load, with rise and fall times on the order of 150 nsec. The positive-bit pulse driver was a Lincoln Laboratory Model VI pulse generator. The two types are identical, except that the Model V delivers a negative pulse, and Model VI delivers a positive pulse.

The fast pulse generator is a Rese Type 1051 millimicrosecond pulse generator. At maximum output, it can drive a 50-ohm load with a 4-amp pulse having rise and fall times of 15 and 25 nsec, respectively. For a 2-amp setting, the rise and fall times are 10 and 18 nsec, respectively. The pulse widths are selected by a switch. The available pulse widths are 10, 20, 50, and 100 nsec.

The timer allows us to operate the equipment in a very flexible manner. A single timer cycle contains eight intervals. Any combination of pulse drivers and scopes may be turned on during each interval. The basic cycle frequency is limited to about 200 cps, because of the long recovery time of the fast pulse generator. An interval stretch option is available which allows us to repeat one interval several times before continuing with the cycle.

Some of the data on the film were taken with a Laboratory-built B-H looper. This device measures the total magnetization of the film as a function of the driving field, and presents the result on an oscilloscope. The axes of the driving field and measured magnetization may be either parallel or perpendicular to each other.

Rather than measure k, we normally measure a quantity H_k, which is the field required to completely rotate the magnetization into the hard direction. For a field less than H_k (if we apply a field in the hard direction only), equating $\overline{M} \times \overline{H}$ to the anisotropy torque gives $uH_h \cos \Lambda = 2k \sin \Lambda \cos \Lambda$. This means that where Λ first reaches 90°, $H_k = 2k/u$. For the plane used, $H_k = 4.3$ oe.

To take the measurement, the field is applied in the hard direction, and the magnetization is measured in the hard direction. The saturation of the flux in the hard direction is spread out due to dispersion so that, usually, H_k is taken to be the value of the field at which a line drawn tangent to the B vs H curve at the origin intersects the saturation value of B.

Dispersion may also be measured with the B-H looper. The plate in the device on which the film is mounted can be rotated. If the driving field is roughly parallel to the easy axis, and the sensing coil perpendicular to the drive coil (see Fig. 11), the magnetization measured by the looper is the difference between the portion of the magnetization to the left and the portion of

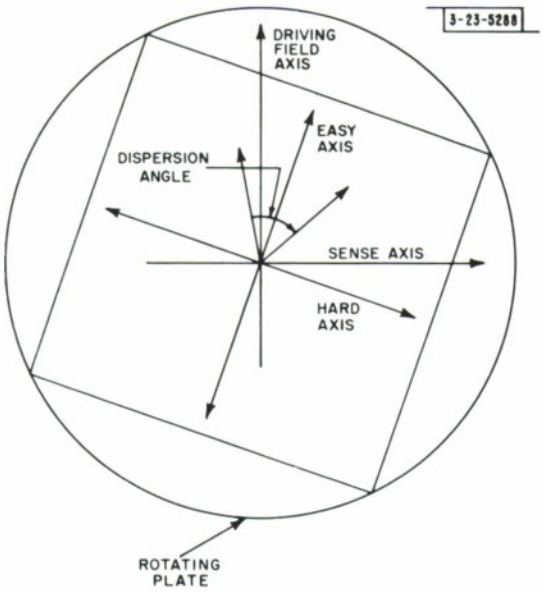

Fig. 11. B-H looper plote mount.

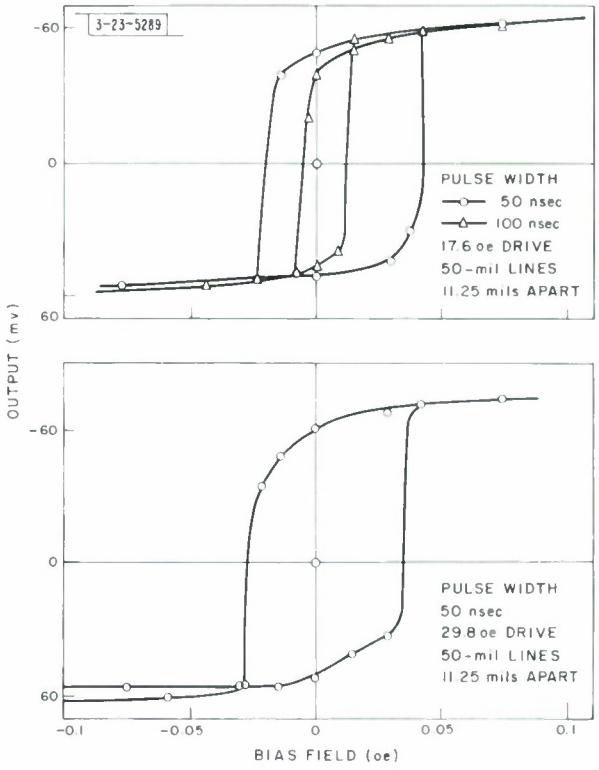

Fig. 12. Bias field vs sense omplifier output hysteresis.

the magnetization to the right of the field axis. This is beeause, under the influenee of the field, the two portions of the magnetization rotate in opposite direetions, and their eomponents along the sense eoil axis eaneel out. The differenee between the two angles where the total magnetization rotates as a unit is the dispersion angle. Normally, the angle between the 90-pereent points is measured.

The magnetization of the film is a eonstant of the material. It is measured by a ferromagnetie resonanee teehnique and has been shown to be 10,000 oe for the material we use. The eomposition of the material is 83-pereent iron and 17-pereent niekel.

The film was evaporated on optieal eover glass in a DC field of 23 oe. It was evaporated for 30 seeonds at an evaporation rate of 1000 Å per minute, giving a thiekness of 500 Å. The field neeessary to produee extensive wall motion in the easy direetion is 1 oe.

V. EXPERIMENTAL PROCEDURE AND RESULTS

At present, there is little data[1] eoneerning eddy eurrent-NDRO in the literature. Therefore, rather than take extensive sets of readings for a single system (varying only one or two parameters) it seemed wiser to eoneentrate on varying several of the parameters, taking less extensive data for eaeh one. Two types of experiments were made.

The first experiment was performed to demonstrate the possibility of eddy-NDRO. We eontinually pulsed the word line, monitoring the output of the sense-amplifier and varying the DC bias produeed by the bit line. If we started with a high positive value of bias and gradually dereased it, the bit would initially be set in the positive direetion. Making the bias negative enough will reverse the direetion of the bit. The same proeedure ean be followed going from a negative to a positive bias. When the results were plotted, a hysteresis loop was observed. This means that there is a range of operating eonditions over whieh the system output has two stable values (depending on history), and NDRO is possible (see Fig. 12).

The signals for large bias levels, for whieh NDRO is impossible, eorrespond to eomplete, eoherent rotation of flux. For the larger loops, there is very little deerease in output in the eddy-NDRO mode. The smaller loop displays a greater signal loss. (We are probably approaeheing the limit at whieh NDRO ean be obtained in this ease.)

When the bias was redueed to zero, the signals appeared perfeetly stable, with no measurable ehange after several million read operations. NDRO at zero bias eould be obtained with all the eonfigurations that were tried. Although no detailed data were taken, the effeets of bit regeneration were noted. If, for example, a bit set in the positive direetion was given a negative bias of suffieient value to eause the signal output to deerease appreeiably (due to break-up), the output signal would inerease again as the eddy eurrent field regenerated the bit – upon reduetion of the magnitude of the negative bias.

The seeond experiment was done to obtain more detailed information about the switehing proeess. We attempted to measure the eddy field as a funetion of time. This is a rather diffieult measurement sinee the fields are small, deeay rapidly, and eoexist with the word drive field (whieh is mueh larger in magnitude). The method finally ehosen is rather indireet. Consider a bit whieh is set in the positive direetion. With a small DC field in the negative direetion, a word pulse is applied. At the end of the word pulse, the effeetive field in the easy direetion is the differenee between the eddy and the bias fields. If the eddy field is larger than the bias field, the magnetization will fall baek in the positive direetion and the sense signal on the trailing edge

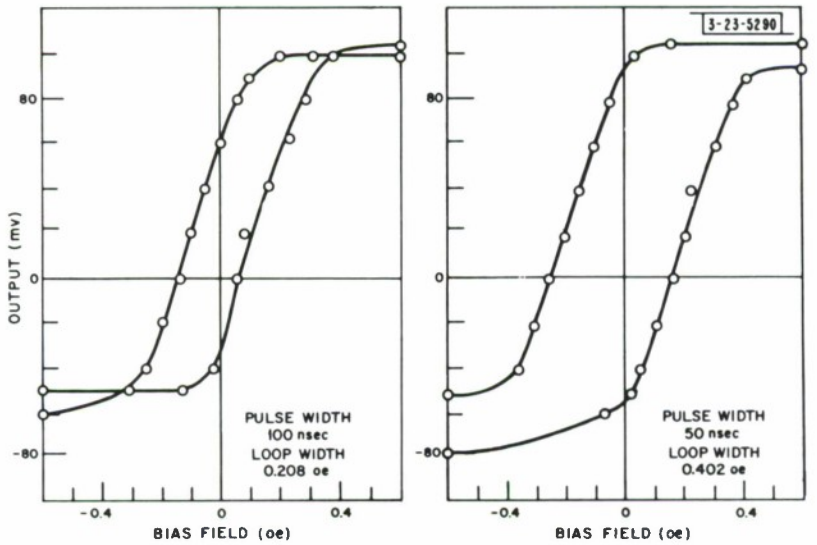

Results		System Porometers	
Time constont	76 nsec	Spacing	7. 25 mils
90-percent transition width	0. 38 oe	Line width	50 mils
Normolized coefficient	0. 143	Driving field	17. 8 oe

Fig. 13. Bias field vs sense amplifier output, eddy field meosurement.

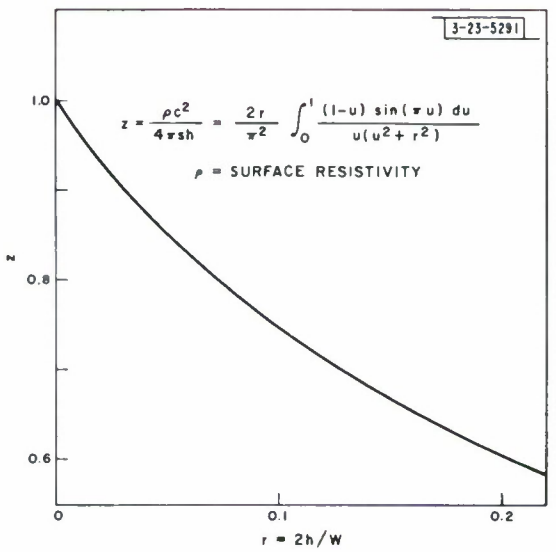

Fig. 14. Normalized time constant for thin, finite striplines

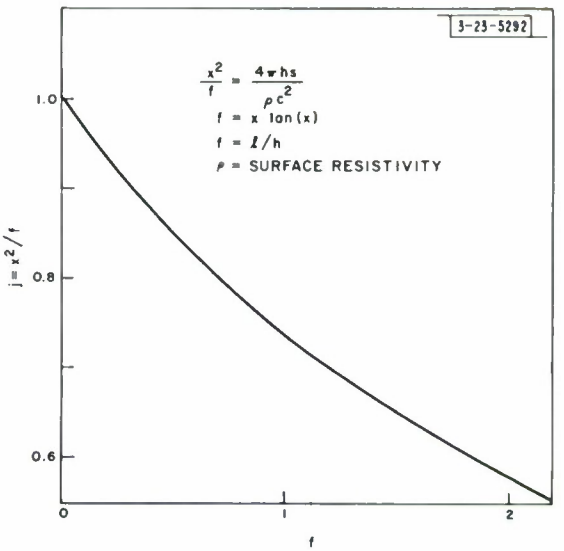

Fig. 15. Inverse normalized time canstant for thick, infinite sheet.

of the word pulse will have a polarity opposite to that of the signal on the leading edge of the word pulse. If the bias field is larger, the polarities will be the same. If the bit were set in the negative direction, a similar transition would occur for positive values of bias. Measuring the difference between the two transitions gives twice the effective eddy field (see Fig. 13).

It would have been better to apply the field in the easy direction only for the short time that the word drive was on, rather than apply it in a DC manner. This is because some wall motion may occur during the time between the writing and reading of the pulse, due to the influence of the DC bias field. The coupling between the bit and sense lines is large enough, however, so that the sense amplifier does not recover for a considerable period of time after the application of the easy direction field, if it is done in a pulsed manner. The effects of wall motion would be indicated by a decrease of the signal obtained on the leading edge of the word pulse with an increase in bias. This effect was not noted for fields on the order of those needed to produce the transitions.

The measurement suffers from several inaccuracies. The poor signal-to-noise ratio made the reading of the output signal value difficult. Also, the dispersion of the bit spread out the transition. The noise could be lowered by reducing the word drive. Reducing the word drive, however, makes the assumption that the bit magnetization is completely switched into the hard direction on the leading edge of the word drive pulse less valid. The value chosen was a compromise. From Fig. 12, it can be seen that there is little change in the hysteresis loops when the driving field is increased from 17.6 to 29.8 oe. The shape of the loops is greatly affected by the size of the eddy field. This verifies the fact that the easy-to-hard-direction switching time is not important for fields much larger than H_k, which is 4.3 oe. For drive fields of the order of H_k, the output signal does decrease.

There is some error due to the neglect of the interaction between neighboring bits. This error amounts to only 0.03 oe, or less, and would be a constant for any experiment, i.e., it merely shifts the zero.

The rise time of the driving pulse is not zero. However, our times are the differences between the 50- and 100-nsec readings. The correction for the finite rise and fall times will increase both values, keeping the difference roughly constant.

The measured values of ρ were found to be 6.5×10^{-4} ohm per square for the 50-mil lines, and 5.37×10^{-4} ohm per square for the 150- and 75-mil lines. Using these values, we calculate the theoretical results shown in Table I. The theoretical values for the thin, finite-width stripline approximation b = 0 were found from (25) and (26) using Fig. 14 (which is a normalized plot of these equations). The theoretical values for the thick, infinite-width sheet approximation $a' = 0$ are found from (3) using Fig. 15.

The experimental results are shown in Table II. The estimated accuracy of the individual eddy field measurements is ±10 percent, and of the time constant, ±30 percent. It is expected that the actual time constant of the slowest decaying mode will be greater than the value calculated by the thin, finite-width sheet approximation and smaller than the value calculated by the infinite-width sheet approximation. The measured time constant would be less than the actual time constant of the slowest decaying mode because of the presence of higher order modes. This is seen to be the case. The thin, finite-width sheet approximation seems to be the better approximation to the actual behavior of the system.

TABLE I

THEORETICAL VALUES

Line Width (mils)	Separation			b (mil^{-1})
	7.25 mils	11.25 mils	14 mils	
Thin, Infinite-Width Sheet [Eq.(4)]				
50	178	272		
75	217	336		
150	217	336		
Thin, Finite-Width Striplines [Eqs.(25), (26)]				
50	120	160	182	0
75	165	225		0
150	191	272		0
50	167			0.0628
Thick, Infinite-Width Sheet, $o' = 0$ [Eq.(3)]				
50	212	305		
75	259	376		
150	259	376		

TABLE II

EXPERIMENTAL RESULTS

Drive (oe)	Width (mils)	Spacing (mils)	Time Constont (nsec)	Normolized Coefficient
13.5	150	7.25	198	0.202
13.5	75	7.25	120	0.208
17.8	50	7.25	76	0.143
17.8	50	11.25	133	0.099

Along with the time constant, the coefficient of the exponential decay is required. It would be possible to find this using the theory that has been presented by doing the detailed linear superposition of normal modes. This involves a very extensive calculation which has not yet been made. Instead, let us obtain an upper bound on the coefficient. Assume that, upon switching the bit magnetization into the hard direction, all of the bit flux is trapped in the copper by the eddy currents, so that the initial eddy flux is the total flux of the bit. Also assume that the entire flux pattern decays with the time constant of the lowest order mode (and that no fast decay process takes place). Finally, assume that there is no fringing, i.e., that the field is uniform across the separation of the word lines and does not extend in the x- and y-directions beyond the borders of the bit. In this case the coefficient of the exponential decay will be ud/2h, where d is the thickness of the bit and u is its magnetization. The actual measured value of the coefficient divided by ud/2h is given in the fifth column of Table II. As can be seen, this is much less than 1, due to the effects of the fringing of the eddy field and the fact that much of the bit flux engages in a rapid decay process. The variation is, as expected, decreasing for structures with large values of 2h/W, and increasing to a limit for those structures for which there is a large overlap of the striplines over the bit.

If the normalized coefficient were 1, the initial value of the normalized eddy field would be:

Spacing (mils)	ud/2h (oe)
7.25	2.72
11.25	1.75

For the structure of two 50-mil word lines separated by 11.25 mils, NDRO is just possible at 100 nsec – as is evidenced by the smallest loop of Fig. 12. The eddy field at the end of the word pulse in this case is 0.0818 oe. This is less than the dispersion from the easy axis, which is 0.172 oe at the 90-percent point. This is not unreasonable since most of the magnetization is quite close to the easy axis, and the 90-percent point is well out on the tail of the dispersion curve. Also, some breakup does occur in this case. We are able to obtain another estimate of the dispersion from the width of the transition. From the 100-nsec curves associated with the structure with 7.25-mil spacing and 50-mil-wide lines, we find that 90-percent dispersion from the easy axis occurs for a field of 0.186 oe. This agrees well with the looper value.

VI. SUGGESTIONS FOR FURTHER STUDY

The work reported here must be considered as representing an initial investigation into a complex phenomenon. Much more remains to be done.

To obtain the maximum amount of information from the theory, the detailed linear superposition of normal modes should be performed. It would be very interesting to see if the low value of the normalized coefficient can be explained by the rapid decay of higher order modes, as has been conjectured. The inclusion of the higher order modes should also bring the measured and calculated values of the time constant into closer agreement. It would also be very useful if a simple means of taking into account both finite stripline thickness and width could be found.

When a better understanding of the details of the decay has been obtained, we can substitute back into (1) to find the dynamic switching behavior of the bit. Some preliminary calculations were performed assuming a simple exponential decay for $f(\rho)$. In agreement with Smay,[3] it is

found that the eddy field will produce resistive damping if the time constant of the eddy field is much less than the rise time of the driving field. If the time constant of the eddy field is much larger than the rise time of the driving field, the eddy field has an instantaneous value which is just proportional to the negative of the change in bit magnetization and has a clamping effect on the switching of the bit. During the short time it takes the bit to switch, the eddy field still decays rapidly, due to the higher order modes. The effective decay time might be short enough to bring us into a range where this decay time is of the same order of magnitude as the rise time of the driving field, and neither of the preceding approximations to (1) are adequate.

The experimental setup could also be improved. With a more flexible pulse generator and a sense amplifier with a wider bandwidth, it might be possible to do a fairly complete job of plotting the eddy field vs time. The use of a bit with smaller dispersion would also increase the accuracy of the measurement. Finally, a most interesting experiment would be to attempt the construction of a prototype eddy-NDRO memory.

ACKNOWLEDGMENT

I wish ta acknowledge the help and encouragement given me by Graup 23, Lincoln Laboratory. In particular, I wish to thonk Jack I. Raffel, Allan H. Andersan and Gilbert Gagnon for their beneficial answers to my numerous questians, and Thamas Crowther for supplying the samples used. I would alsa like ta express my gratitude to the thin film memory graup af the Bordman Road Laboratories, I.B.M., Poughkeepsie, New York, where I first became interested in the prablem.

I greatly appreciate the understanding and effort of my thesis advisar, Dr. Alan L. McWhorter.

REFERENCES

1. R.H. Tancrell, "Thin Ferromognetic Films as Functian Table Elements," M.Sc. Thesis, Massachusetts Institute af Technology (1958).
2. J.M. Daughton, J.A. Smay, A.V. Pohm, ond A.A. Read, J. Appl. Phys. Suppl. 32, 36S (1961).
3. T.A. Smoy, "Energy Transfer Properties of Thin Magnetic Film Logical Elements," Ph. D. Thesis, Iowa Stote University af Science and Technology (1962).
4. F.B. Hildebrandt, Methods of Applied Mathematics (Prentice-Hall, New Jersey, 1952), pp.1-100.
5. Y.W. Lee, Statistical Theary af Cammunication (Wiley, New York, 1960), pp.476-478.
6. "Standard Test Equipment," Report 6R-215, Section 28, Lincoln Labaratary, M.I.T. (1 December 1957).

APPENDIX A

Since I_z is zero in regions I and III,

$$\frac{Ho'y}{Ho'x} = \frac{Ho'''y}{Ho'''x} = -\frac{b}{g} = \frac{Ho''y}{Ho''x} \quad . \tag{A-1}$$

Substituting (A-1) into the relations derived from $\nabla \cdot \overline{H} = 0$ gives

$$a''Ho''z = \left(\frac{b^2}{g} + g\right) Ho''x \quad , \tag{A-2}$$

$$a'Ho'''z = \left(\frac{b^2}{g} + g\right) Ho'''x \quad , \tag{A-3}$$

$$a'Ho'z = -\left(\frac{b^2}{g} + g\right) Ho'x \quad . \tag{A-4}$$

The boundary conditions at z = h give

$$Ho''z \sin(a''h + n) = \sinh(a'h)\, Ho'''z \quad , \tag{A-5}$$

$$Ho''x \cos(a''h + n) = \cosh(a'h)\, Ho'''x \quad . \tag{A-6}$$

Dividing (A-5) by (A-6) and using (A-3) and (A-4) gives

$$\frac{1}{a''} \tan(a''h + n) = \frac{1}{a'} \tan(a'h) \quad . \tag{A-7}$$

At $z = h + \ell$ we find

$$Ho'z \exp[-a'(h + \ell)] = Ho''z \sin[a''(h + \ell) + n] \quad , \tag{A-8}$$

$$Ho'x \exp[-a'(h + \ell)] = Ho''x \cos[a''(\ell + h) + n] \quad . \tag{A-9}$$

Dividing (A-8) by (A-9) and applying (A-2) and (A-3) gives

$$\tan[a''(h + \ell) + h] = -\frac{a''}{a'} \quad . \tag{A-10}$$

Using (A-10) and (A-7), we can eliminate n and find a relation between a'', h, ℓ, and a':

$$(a'/a'') \tan(a''\ell) = \frac{\tanh(a'h) + 1}{(a''/a')^2 \tanh(a'h) - 1} \quad .$$

APPENDIX B

Consider Eq. (10). Apply Eqs. (13) and (14) and divide out the sinusoidal variation in y. We find (10) becomes

$$\sum_{n=0}^{\infty} A_n \frac{2}{c} \int_{-g/2}^{g/2} dx' \frac{(x - x') \, Co(b\lambda) \sin(\frac{Nbx'}{g}) - \frac{g\lambda}{N} \cos(\frac{Nbx'}{g}) \, So(b\lambda)}{\lambda^2} \quad .$$

We multiply through by cos (Qbx/g) and integrate from $-W/2$ to $W/2$. It is convenient to do the integral from $-g/2$ to $g/2$, integrating with respect to u = bx. Define u' = bx'. The expression becomes

$$\sum_{n=0}^{\infty} A_n \frac{2}{cb} \int_{g/2}^{g/2} du \int_{-g/2}^{g/2} du' \frac{[(u - u') \, Co(b\lambda) \sin(\frac{Nu'}{g}) - \frac{bg\lambda}{N} \cos(\frac{Nu'}{g}) \, So(b\lambda)] \cos(\frac{Qu}{g})}{b\lambda^2} \quad .$$

We now define $u - u' = k$; $du' = -dk$. Since λ is only a function of K, we may do the integral with respect to u in closed form. Since changing the sign of both u and u' does not change the value of the integrand, we need only consider positive values of K and multiply the answer by 2. The expression we must integrate becomes

$$\sum_{n=0}^{\infty} A_n \frac{2}{cb} \int_{o}^{g} dk \int_{-g/2+k}^{g/2} du$$

$$\times \frac{2 \{K \sin[\frac{N}{g}(u - K)] \, Co(b\lambda) - \frac{bg\lambda}{N} \cos[\frac{N}{g}(u - K)] \, So(b\lambda)\} \cos(\frac{Qu}{g})}{b\lambda^2} \quad . \qquad (B\text{-}1)$$

It is elementary to show that if q is not equal to n:

$$\int_{-g/2}^{g/2} du \sin[\frac{N}{g}(u - K)] \cos(\frac{Qu}{g}) = -\frac{g}{2} \left[\frac{\cos(\frac{Q + N}{g} u - \frac{N}{g} K)}{N + Q} \right.$$

$$\left. + \frac{\cos(\frac{N - Q}{g} u - \frac{N}{g} K)}{N - Q} \right] \Bigg|_{-g/2+K}^{g/2} ,$$

$$\cos(\frac{Q + N}{g} \cdot \frac{g}{2}) = \cos[\frac{\pi(2n + 2q + 2)}{2}] = -\cos \pi(n + q) \quad ,$$

$$\cos(\frac{Q - N}{2}) = \cos(\frac{N - Q}{2}) = \cos \pi(n - q) \quad .$$

If $n - q$ is odd, $n + q$ is also. If $n - q$ is even, so is $n + q$. Therefore,

$$\cos(\frac{N - Q}{2}) = (-1)^{n-q} = -\cos(\frac{N + Q}{2}) \quad ,$$

$$\sin(\frac{N - Q}{2}) = \sin(\frac{N + Q}{2}) = 0 \quad .$$

Applying these results, and computing the value of the integral, we find

$$\int_{-g/2+K}^{g/2} du \sin[\frac{N}{g}(u - K)] \cos\frac{Qu}{g} = \frac{2g(-1)^{n-q} Q}{Q^2 - N^2} \sin(\frac{N + Q}{2g} K) \sin(\frac{Q - N}{2g} K) \quad .$$

In a similar manner, it can be shown

$$\int_{-g/2+K}^{g/2} du \cos\left[\frac{N}{g}(u-K)\right]\cos\left(\frac{Qu}{g}\right) = \frac{W(-1)^{n-q}}{Q^2-N^2}\left[N\sin\left(\frac{QK}{W}\right) - Q\sin\left(\frac{NK}{W}\right)\right] \quad .$$

If n = q, we find

$$\int_{-g/2+K}^{g/2} du \cos\left(\frac{Qu}{g}\right)\sin\left[\frac{Q}{g}(u-K)\right] = \frac{K-g}{2}\sin\frac{Q}{g}K \quad ,$$

$$\int_{-g/2+K}^{g/2} du \cos\left(\frac{Qu}{g}\right)\cos\left[\frac{Q}{g}(u-K)\right] = \frac{g-K}{2}\cos\left(\frac{QK}{g}\right) + \frac{g}{2Q}\sin\left(\frac{KQ}{g}\right) \quad .$$

We may now apply these results to (B-1). First we rewrite (B-1) as

$$\frac{1}{cb}\sum_{n=0}^{\infty} A_n H_{nq}^{1}(b) \quad ; \tag{B-2}$$

$$H_{nq}^{1}(b) = 4\int_0^g \frac{(-1)^{n-q}\,gdK}{b\lambda^2(Q^2-N^2)}\left\{2QK\,Co(b\lambda)\sin\left[\frac{Q+N}{2g}K\right]\sin\left[\frac{Q-N}{2g}K\right]\right.$$

$$\left. + \left[Q\sin\left(\frac{NK}{g}\right) - N\sin\left(\frac{QK}{g}\right)\right]\frac{gb\lambda}{N}\,So(b\lambda)\right\} \quad ,$$

$$H_{qq}^{1}(b) = 4\int_0^g dK\,\frac{\frac{K(K-g)}{2}\,Co(b\lambda)\sin\left(\frac{QK}{g}\right) - \frac{gb\lambda}{N}\,So(b\lambda)\,I(K)}{b\lambda^2} \quad ,$$

$$I(K) = \frac{g-K}{2}\cos\left(\frac{QK}{g}\right) + \frac{g}{2Q}\sin\left(\frac{QK}{g}\right) \quad .$$

There is also a contribution to H_z from the current in the upper sheet. The computations for this integral are the same as for the one already done if we set m = 0, except that the sign is opposite because the currents in the upper stripline are the negative of the currents in the lower stripline. If m is zero, λ becomes merely k/b.

For the upper stripline currents, the expression corresponding to (B-2) is

$$\frac{1}{cb}\sum_{n=0}^{\infty} A_n H_{nq}^{u}(b) \quad ; \tag{B-3}$$

$$H_{nq}^{u}(b) = -4\int_0^g \frac{(-1)^{n-q}\,gdKb}{K(Q^2-N^2)}\left\{2Q\,Co(K)\sin\left(\frac{Q+N}{2g}K\right)\sin\left(\frac{Q-N}{2g}K\right)\right.$$

$$\left. + \left[Q\sin\left(\frac{NK}{g}\right) - N\sin\left(\frac{QK}{g}\right)\right]\frac{g}{N}\,So(K)\right\} \quad ,$$

$$H_{qq}^{u}(b) = 4\int_0^g \frac{bdK\left[\frac{g}{N}\,So(K)\,I(K) - \frac{K-g}{2}\,Co(K)\sin\left(\frac{QK}{g}\right)\right]}{K} \quad .$$

Therefore, we find that after dividing out the sinusoidal dependence on y, multiplying by cos (Qbx/g), and integrating from −W/2 to W/2, Eq. (7) reduces to

$$\frac{1}{bc} \sum_{n=0}^{\infty} A_n H_{nq}(b) \quad , \tag{B-4}$$

$$H_{nq}(b) = 4 \int_o^g \frac{(-1)^{n-q}\, g dK}{K\lambda^2 (Q^2 - N^2)} \{2Q \sin(\frac{Q+N}{2g} K) \sin(\frac{Q-N}{2g} K) D_c$$

$$+ [N \sin(\frac{QK}{g}) - Q \sin(\frac{NK}{g})] \frac{g}{N} D_s\} \quad ,$$

$$H_{qq}(b) = 4 \int_o^g \frac{dK}{K\lambda^2} \left\{ \frac{g}{N} [b\lambda^2 So(K) - K So(b\lambda)] I(K) \right.$$

$$\left. + \frac{K-g}{2} \sin(\frac{QK}{g}) \left[\frac{K^2}{b} Co(b\lambda) - b\lambda^2 Co(K) \right] \right\} \quad .$$

We now consider $(\nabla \times \bar{J}) \cdot \bar{1}_z (\rho c/s)$ and execute the same operations applied to (7). From (9),

$$\frac{\rho c}{s} \bar{1}_z \cdot (\nabla \times \bar{J}) = b \frac{\rho c}{s} \sum_{n=0}^{\infty} A_n (\frac{N}{g} + \frac{g}{N}) \cos(\frac{Nbx}{g}) \sin(by) \quad .$$

Dividing by $\sin(by)$, multiplying by $\cos(Qbx/g)$, and integrating:

$$\frac{b\rho c}{s} \sum_{n=0}^{\infty} A_n (\frac{N}{g} + \frac{g}{N}) \int_{-g/2}^{g/2} \cos(\frac{Nbx}{g}) \cos(\frac{Qbx}{g}) du = \frac{b\rho c}{s} \frac{g}{2} A_\rho (\frac{Q}{g} + \frac{g}{Q}) \quad .$$

Therefore, with $H_{nq}(b)$ given by (B-4):

$$\frac{\rho c^2 Q b^2}{2s} [1 + (\frac{g}{Q})^2] A_\rho = \sum_{n=0}^{\infty} A_n H_{nq}(b) \quad . \tag{B-5}$$

Security Classification

DOCUMENT CONTROL DATA - R&D

(Security classification of title, body of abstract and indexing annotation must be entered when the overall report is classified)

1. ORIGINATING ACTIVITY *(Corporate author)*

LINCOLN LABORATORY M. I. T.
LEXINGTON, MASS.

2a. REPORT SECURITY CLASSIFICATION

UNCLASSIFIED

2b. GROUP N/A

3. REPORT TITLE

NONDESTRUCTIVE READOUT SCHEME FOR THIN FILM MEMORIES

4. DESCRIPTIVE NOTES *(Type of report and inclusive dates)*

5. AUTHOR(S) *(Last name, first name, initial)*

MALTZ, M. S.

6. REPORT DATE	7a. TOTAL NO. OF PAGES	7b. NO. OF REFS
21 MAY 1964	35	6

8a. CONTRACT OR GRANT NO.	9a. ORIGINATOR'S REPORT NUMBER(S)
AF 19(628)-500	TR 355
b. PROJECT NO.	
c.	9b. OTHER REPORT NO(S) *(Any other numbers that may be assigned this report)*
d.	ESD-TDR-64-333

10. AVAILABILITY/LIMITATION NOTICES

QUALIFIED REQUESTORS MAY OBTAIN FROM DDC.
OTS RELEASE AUTHORIZED

11. SUPPLEMENTARY NOTES	12. SPONSORING MILITARY ACTIVITY
	HQ ESD L. G. HANSCOM FIELD BEDFORD, MASS. 01731

13. ABSTRACT

If a magnetic bit in a thin film memory array is driven in the hard direction, the changing flux produces eddy currents in the surrounding conducting surfaces. It has been pointed out by Pohm and others that the eddy field produced by these currents always tends to restore the bit magnetization to its original direction. If this eddy field were strong enough at the end of the word drive pulse, the effect could be made the basis of a scheme for nondestructive readout (NDRO). Some experiments were performed on structures where the eddy field was strong enough to restore the bit. The thin film plane used contained 50 X 50-mil X 500-A-thick Permalloy films with uniaxial anisotropy. The word line was completely wrapped around the plane. Word-line-to-word line spacings of 11.25 and 7.25 mils, and word-line widths of 50, 75, and 150 mils were used. The eddy field was measured at 50 and 100 nsec after the switching operation and, assuming an exponential eddy field decay, a time constant was calculated. Two theoretical approximations were considered. In both, the eddy currents were assumed to flow only in the word lines. In one, the thickness of the lines was assumed negligible. In the other approximation, the thickness of the striplines was considered, but was assumed to be of infinite width. The finite width, thin stripline approximation seems to be in better agreement with the measured values of the time constant which varies between 76 and 200 nsec.

DD FORM 1 JAN 64 1473

Security Classification

14. KEY WORDS	LINK A		LINK B		LINK C	
	ROLE	WT	ROLE	WT	ROLE	WT
MEMORY DEVICES MAGNETIC FILM THIN FILM READOUT EDDY CURRENTS MATHEMATICAL ANALYSIS EQUATIONS						

INSTRUCTIONS

1. ORIGINATING ACTIVITY: Enter the name and address of the contractor, subcontractor, grantee, Department of Defense activity or other organization *(corporate author)* issuing the report.

2*a*. REPORT SECURITY CLASSIFICATION: Enter the overall security classification of the report. Indicate whether "Restricted Data" is included. Marking is to be in accordance with appropriate security regulations.

2*b*. GROUP: Automatic downgrading is specified in DoD Directive 5200.10 and Armed Forces Industrial Manual. Enter the group number. Also, when applicable, show that optional markings have been used for Group 3 and Group 4 as authorized.

3. REPORT TITLE: Enter the complete report title in all capital letters. Titles in all cases should be unclassified. If a meaningful title cannot be selected without classification, show title classification in all capitals in parenthesis immediately following the title.

4. DESCRIPTIVE NOTES: If appropriate, enter the type of report, e.g., interim, progress, summary, annual, or final. Give the inclusive dates when a specific reporting period is covered.

5. AUTHOR(S): Enter the name(s) of author(s) as shown on or in the report. Enter last name, first name, middle initial. If military, show rank and branch of service. The name of the principal author is an absolute minimum requirement.

6. REPORT DATE: Enter the date of the report as day, month, year; or month, year. If more than one date appears on the report, use date of publication.

7*a*. TOTAL NUMBER OF PAGES: The total page count should follow normal pagination procedures, i.e., enter the number of pages containing information.

7*b*. NUMBER OF REFERENCES: Enter the total number of references cited in the report.

8*a*. CONTRACT OR GRANT NUMBER: If appropriate, enter the applicable number of the contract or grant under which the report was written.

8*b*, 8*c*, & 8*d*. PROJECT NUMBER: Enter the appropriate military department identification, such as project number, subproject number, system numbers, task number, etc.

9*a*. ORIGINATOR'S REPORT NUMBER(S): Enter the official report number by which the document will be identified and controlled by the originating activity. This number must be unique to this report.

9*b*. OTHER REPORT NUMBER(S): If the report has been assigned any other report numbers *(either by the originator or by the sponsor)*, also enter this number(s).

10. AVAILABILITY/LIMITATION NOTICES: Enter any limitations on further dissemination of the report, other than those imposed by security classification, using standard statements such as:

(1) "Qualified requesters may obtain copies of this report from DDC."

(2) "Foreign announcement and dissemination of this report by DDC is not authorized."

(3) "U. S. Government agencies may obtain copies of this report directly from DDC. Other qualified DDC users shall request through

_____."

(4) "U. S. military agencies may obtain copies of this report directly from DDC. Other qualified users shall request through

_____."

(5) "All distribution of this report is controlled. Qualified DDC users shall request through

_____."

If the report has been furnished to the Office of Technical Services, Department of Commerce, for sale to the public, indicate this fact and enter the price, if known.

11. SUPPLEMENTARY NOTES: Use for additional explanatory notes.

12. SPONSORING MILITARY ACTIVITY: Enter the name of the departmental project office or laboratory sponsoring *(paying for)* the research and development. Include address.

13. ABSTRACT: Enter an abstract giving a brief and factual summary of the document indicative of the report, even though it may also appear elsewhere in the body of the technical report. If additional space is required, a continuation sheet shall be attached.

It is highly desirable that the abstract of classified reports be unclassified. Each paragraph of the abstract shall end with an indication of the military security classification of the information in the paragraph, represented as *(TS)*, *(S)*, *(C)*, or *(U)*.

There is no limitation on the length of the abstract. However, the suggested length is from 150 to 225 words.

14. KEY WORDS: Key words are technically meaningful terms or short phrases that characterize a report and may be used as index entries for cataloging the report. Key words must be selected so that no security classification is required. Identifiers, such as equipment model designation, trade name, military project code name, geographic location, may be used as key words but will be followed by an indication of technical context. The assignment of links, rules, and weights is optional.